35th EPS Conference on Plasma Phys. Hersonissos, 9 - 13 June 2008 ECA Vol.**32D**, P-4.048 (2008)

Modeling of confinement improvement and impurity transport in high power JET discharges with neon seeding

S.Moradi[1], M.Tokar[2], D.Kalupin[2], H.Nordman[3], R.Singh[4], B. Weyssow[5]
and the JET-EFDA Contributors*
JET-EFDA, Culham Science Centre, OX14 3DB, Abingdon, UK

[1]*Department of statistical and plasma physics, Universite libre de Bruxelles, Brussels, Belgium*
[2] *Institute for Plasma Physics, Forschungszentrum Juelich GmbH, Jülich, Germany*
[3] *Department of Radio and Space Science, Chalmers University of Technology, Euratom-VR Association, SE-412 96 Goteborg, Sweden*
[4]*Institute for Plasma Research, Bhat, Gandhinagar-382 428, India*
[5]*Department of statistical and plasma physics, Universite libre de Bruxelles, Brussels, Belgium, EFDA-CSU Garching, München Germany*
See the Appendix of M.L.Watkins et al., Fusion Energy 2006 (Proc. 21st Int. Conf. Chengdu, 2006) IAEA, (2006)

I. Introduction

Deliberate seeding of impurities has been applied on several fusion devices [1] in order to create a strongly radiating boundary, distributing the power transported from the plasma core on a larger wall area, and to reduce head loads on limiters and divertor target plates. Under conditions of the low (L) confinement mode [2] simultaneous reduction of the anomalous transport of particles and energy and transition to the so called radiative improved (RI) mode has been achieved on TEXTOR [3]. By puffing of argon impurity a noticeable confinement improvement has been also seen in the high (H) confinement mode in the divertor tokamak JT-60U. However, earlier analogous experiments on JET [4] did not lead to the desirable result and suffer, when argon concentration exceeded some critical level, from unwanted and uncontrollable impurity accumulation in the plasma core with strongly peaked core radiation and flat temperature profile.

In recent JET campaigns in 2006-2007 neon seeding in JET plasmas with a very high heating power of 30 MW has been explored [5]. The obtained discharge conditions reveal several important benefits for a fusion reactor: (i) the radiated power fraction up to 60%, providing significant reduction of power fluxes to the target tiles; (ii) the strong reduction of the amplitude of the edge localized modes, and (iii) the transport reduction seen in the formation of an edge pedestal on the ion temperature profile and its increase in the plasma core, from 6 to 12 keV. Important that the neon concentration profile, as measured by the charge exchange recombination spectroscopy, is hollow with a concentration of about 1% in the core rising to $\sim 2.5\%$ at the normalized radius of 0.7. No signs of impurity accumulation have been found in these discharges [5]. In this work two discharges, 69093 and 69092 have been considered, with high and low content of neon seeded into plasmas with a very high heating power of 30 MW at $q_{95} \sim 5$ and high triangularity, δ (relevant to the ITER steady-state demonstration) reaching $\beta_N \sim 2$ with ITER-AT magnetic configuration, $B_0 \sim 3.1T, I_P \sim 1.9MA$. The discharges were part of the experiments devoted to impurity injection (for ELM mitigation purposes) in AT scenarios which are H-modes with non-standard current profiles, of the type that has been seen to promote confinement improvement through the formation of ITBs. We performed a predictive transport modeling of the JET plasma conditions describe above and provide an explanation for the confinement improvement achieved with neon seeding.

II. Predictive transport modeling with code RITM

For predictive transport modeling of JET plasmas seeded with impurities the one-dimensional transport code RITM [6, 7, 8] has been applied. The RITM code allows a self-consistent description of heat and particle transport in the entire cross section of the plasma from the axis to the separatrix. The plasma shaping is taken into account by using the Shafranov shift calculated with inductively driven and bootstrap contributions to the current density and prescribed elongation

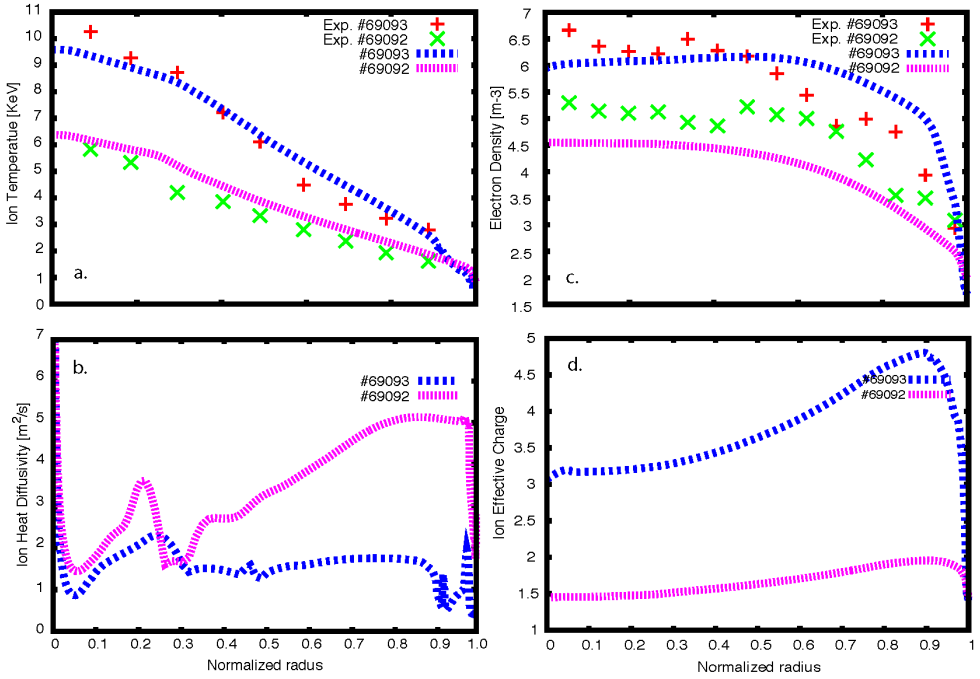

Figure 1: Profiles of ion temperature, ion heat diffusivity, electron density, and ion effective charge versus the normalized radius ρ calculated and measured in shot 69092 with low neon content (pink curve and green crosses, respectively) and 69093 with high neon concentration (blue curve and red pluses, correspondingly).

and triangularity of magnetic surfaces. Continuity equations for the electrons and impurity ions in all ionization stages are solved, including diffusive and convective components of the particle fluxes. The charged particle sources are determined by taking into account the ionization of neutrals generated by neutral beam injection (NBI) and those entering the confined volume across the separatrix. The behavior of the latter in the plasma is described in the diffusive approximation. The flux and density of the background ions is calculated under the assumption of the plasma quasi-neutrality. The external fueling rates of background neutrals and of neon atoms are adapted to match the experimental volume average electron density and the total radiated power inside the confined plasma. The radiation profile is computed by taking all neon impurity ionization stages into account. This profile then is used together with the experimental profiles of auxiliary heating power density from the NBI and high frequency radiowaves in the ion and electron heat transport equations to calculate the ion and electron temperature profiles. The boundary conditions at the separatrix are defined by the experimental decay lengths of the plasma parameters. The transport model in RITM accounts for the most important drift modes due to toroidal ion temperature gradient (ITG), dissipative trapped electron (DTE), drift-Álfven (DA) and drift resistive ballooning (DRB) instabilities and the transport coefficients computed in mixing length limit [9]. For impurity ions the same anomalous diffusivity as for the main particles and the convection velocity calculated in Ref. [10] accounting for ITG and TE modes in the collisionless limit are used. Besides at the edge we add the neoclassical convective velocity computed according to Ref. [11]. This assumption that the total impurity convection velocity can be considered as the sum of anomalous and neoclassical ones is justified by the fact that neoclassical transport is driven by parallel friction dynamics, and is not affected significantly by the ion cross-field transport which is dominated by fluctuations.

III. Results of calculations for JET plasma conditions

Two discharges, 69093 and 69092 have been considered here, with high and low content of neon seeded respectively. In figure 1 the results of RITM calculations are compared with the experimental data of these discharges for JET. As one can see in figure 1a, the increase in the

ion temperature by strong neon seeding is in relatively good agreement with the experimentally observed one. The causes for this temperature elevation can be understood by analysing figure 1b where the radial profiles of the ion heat diffusivity χ_i are shown. First, χ_i is significantly decreased over the whole plasma radius and, second, the width of the edge transport barrier (ETB) where χ_i is reduced to the neoclassical level is noticeably increased. One can interpret this evolution by taking into account that the main contribution to the anomalous part in χ_i is due to ITG instability. This contribution is determined by the ITG growth rate

$$\gamma_{ITG} \sim \sqrt{\frac{1}{Z_{eff} L_{T_i}} - \frac{1}{L_{T_i}^{cr}}} \tag{1}$$

where L_{T_i} and $L_{T_i}^{cr}$ are the e-folding length of the ion temperature and its critical value, correspondingly. In the plasma core the T_i-profile is stiff, i.e., $Z_{eff} L_{T_i} \approx L_{T_i}^{cr}$ and for relatively flat density $L_{T_i}^{cr} \approx \alpha R$. With a constant Z_{eff} we get $T_i(0)/T_i(r_b) \approx \exp\left(Z_{eff} r_b / \alpha R\right)$ where r_b is the minor radius of the ETB top position. This temperature ratio grows up with increasing Z_{eff}. In the ETB $L_{T_i}^{cr}$ is mostly governed by the very sharp density gradient providing $1/\left(Z_{eff} L_{T_i}\right) < 1/L_{T_i}^{cr}$ and ITG instability is completely suppressed here. The density gradient reduces with the distance from the separatrix, $L_{T_i}^{cr}$ increases and at the ETB top the condition $1/\left(Z_{eff} L_{T_i}\right) = 1/L_{T_i}^{cr}$ is first satisfied. Therefore ETB broadens with increasing Z_{eff}. Computation for the lower neon content have shown that not any prescribed density level can be achieved simply by increasing the intensity of the main gas puffing: increasing neutral influx leads to edge cooling and deterioration of particle confinement through the development of edge instabilities normally suppressed in the ETB. Presently it was not possible to reproduce the experimental density profile accurately enough, see figure 1c, which would probably require some amendments in the transport model. By increasing neon content the particle confinement deterioration can be overcame if the neon influx exceeds a critical level leading to Z_{eff} about 3. Figure 1d displays the radial profile of Z_{eff} calculated by using for impurities the diffusivity of the main ions, anomalous convection determined according to the model of Ref. [10] and neoclassical convection [11] taken into account at the outmost 20 % of the minor radius only. This assumption has been made because the neoclassical convection in this region has pronounced contribution and provides a good level of neon concentration, comparative to observed values, while for the more internal regions causes accumulation of neon in the plasma central region which is in contradiction to experimental observation. In the case with low neon puffing Z_{eff} is lower than 2 everywhere. The Z_{eff}-profile calculated for higher neon content reproduces well several features of the measured profile for Ne^{10+} ion concentration, figure 7 in Ref. [5]: it is hollow in the main part of the plasma radius and at the position of the maximum in the Ne^{10+} concentration at the dimensionless radius of 0.65 both profiles provide roughly Z_{eff} of 3.5. However, the calculated Z_{eff} starts to decline only very close to the separatrix, i.e., in the ETB only. The hollowness of the Z_{eff}-profile in the central plasma is mostly due to nonstationarity of the situation with respect to the impurity density.

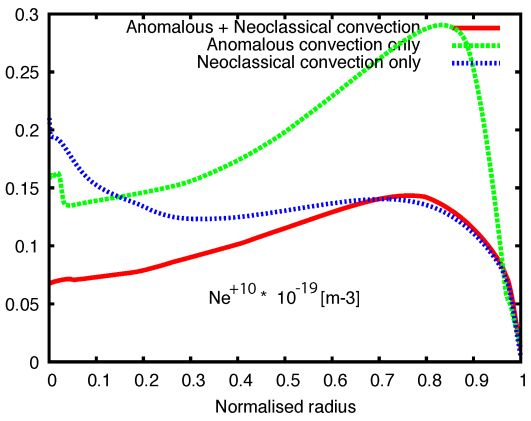

Figure 2: Calculated radial profiles of Ne^{10+} ion density with different assumptions about impurity convective velocity: anomalous plus neoclassical at $0.8 \leq \rho \leq 1$ (red curve), pure anomalous (green curve) and pure neoclassical one (blue curve).

In order to examine the sensitivity to the impurity convection the cases where the anomalous

and neoclassical contributions along were included have been tested. Figure 2 displays the radial profiles of the Ne^{10+} ion density for the conditions of strong neon puff calculated with different assumptions on the impurity convection velocity and the impurity diffusivity the same as that of the main plasma particles. Since the latter is very small in the ETB only a strong enough outward convection can lead to the central neon density in agreement with the experimental one. In the case with anomalous convection only, impurity density grows up to the level significantly exceeding the experimental one. Anomalous transport channel can not provide such a level and the Ne^{10+} density achieved is far too high. Conversely, the neoclassical transport provides in the ETB a positive radial velocity of several m/s, because here Ne^{10+} impurity ions are in the Pfirsch-Schlüter regime and the dominant convection contribution is due to the main ion temperature gradient and is directed outwars. The situation is opposite near the plasma axis where impurities are in the plateau regime and the neoclassical convection is negative. Therefore with pure neoclassical convection a peaking of the Ne^{10+} ion density at the axis occurs. As a consequence the temperature profile flattens in the core in contradiction to experimental observations. Thus the standard neoclassics obviously fails to describe impurity convection in the core of plasmas in question and further development of mpurity transport models is of very importance.

IV. Discussion

The proposed explanation is that the possible confinement improvement through the reduction of anomalous ion transport, caused by increase in Z_{eff} due to neon seeding[12]. There are several major differences in these discharges with respect to previous experiments on JET, with seeding the argon into high density H-mode plasmas: (i) the total heating power is increased up to 30 MW (ii) new divertor geometry (removed septum) and plasma shaping (high triangularity, ITER like plasmas), (iii) substantially modified profile of the safety factor (flat q-profile in the center). The previous modeling showed that the injection of impurities into regular H-mode only weakly affects the background transport [7]. What should also be taken into consideration is that in low confinement shot (69092) the MHD modes have been observed. This can deteriorate confinement, on the other hand, the high confinement shot (69093) potentially has the ITB which might improve the confinement properties. To make a solid conclusion on the mechanism dominating the confinement improvement, the number of discharges taken for the modeling should be extended, with a large variety of plasma conditions, including earlier H-mode discharges with impurity seeding. It is also necessary to consider other mechanisms besides of ITG stabilization, such as MHD or ITB, that might affect the confinement properties.

Acknowledgment

This work, supported by the European Communities under the contract of Association between EURATOM/Belgium state, was carried out within the framework of the European Fusion Development Agreement. The views and opinions expressed herein do not necessarily reflect those of the European Commission.

References

[1] J. Ongena *et al*, Phys. Plasmas **4**, 2188 (2001)
[2] R. R. Dominguez and R. E. Waltz, Nucl. Fusion **27**, 65 (1987)
[3] J. Ongena *et al*, Physics of Plasmas **8**, 2188 (2001)
[4] G. F. Matthews *et al*, Nucl. Fusion **39**, 19 (1999)
P. Dumortier *et al*, Plasma Phys. Control. Fusion **44**, 1845 (2002)
[5] X. Liutadon *et al*, Plasma Phys. Control. Fusion **49**, B529-B550 (2007)
[6] M. Z. Tokar, Plasma Phys. Control. Fusion **36**, 1819 (1994)
[7] B. Unterberg *et al*, Plasma Phys. Control. Fusion **46**, A241 (2004)
[8] D. Kalupin *et al*,Nucl. Fusion **45**, 468 (2005)
[9] J. Weiland, *Collective Modes in Inhomogeneous Plasmas. Kinetic and Advanced Fluid Theory* (Bristol: Institute of Physics Publishing) (2000)
[10] H. Nordman and T. Fülop, Physics of Plasmas **14**, 052303 (2007)
[11] K. W. Wenzel and D. J. Sigmar, Nucl. Fusion **30**, 1117 (1989)
[12] M. Z. Tokar *et al*, Physical Review Letters **84**, 895 (2000)